AN AUGMENTED LAGRANGIAN BASED SHOOTING METHOD FOR THE TRAJECTORY OPTIMIZATION OF SWITCHED LAGRANGIAN SYSTEMS

Kerim Yunt
Center of Mechanics
IMES, ETH Zurich
Switzerland
kerimyunt@gmx.ch
(kerim.yunt@imes.mavt.ethz.ch)

Abstract
The application range of a shooting method based on Moreau's sweeping process is extended to the class of switching Lagrangian systems. The method finds at least quasi-optimal trajectories based on a non-gradient minimization strategy that utilizes the augmented Lagrangian approach.

Key words
measure differential inclusion, Moreau's sweeping process

In this work a shooting method is generalised to a certain class of Lagrangian systems which has first been in studied in [Yunt and Glocker, 2005], and in [Yunt, 2006] the method has been combined with the augmented Lagrangian method and a convergence proof is given. The novel feature is that the method determines the partition and mode sequence in addition to the controls and does not require any gradient information for the class of switching Lagrangian systems. The most common class of switching Lagrangian systems are mechanical systems with stick-slip transitions. In [Murphey 2002] T. Murphey addresses some aspects of non-smooth dynamics of mechanical systems and control aspects are treated. There he introduces the terminology *multiple-model systems*, referring to the fact that through contact interactions such as stick-slip transitions, the mechanical system can be represented by different differential equations depending on the state of the contacts. In the sequel the definition of switching Lagrangian system is given and the concept of hybrid execution is introduced.

Definition Switching Lagrangian Systems A switching Lagrangian systems is defined by the following properties:

1. A set of discrete modes $\mathcal{I}_M$
2. For each $l \in \mathcal{I}_M$, manifold $\mathcal{M}_\mathrm{l}$, with boundary $\partial\mathcal{M}_\mathrm{l}$ if it exists, and a Lagrangian function $\mathcal{L}_\mathrm{l} : \mathcal{T}\,\mathcal{M}_\mathrm{l} \to \mathbb{R}$ defined on the tangent bundle of $\mathcal{M}_\mathrm{l}$, where the domains $\mathcal{M}_\mathrm{l}$ are disjoint.
3. A set of discrete transitions $\mathcal{E}_\mathrm{T} \subset \mathcal{I}_M \times \mathcal{I}_M$;
4. For each discrete transition, there exists a set-valued force law that relates the velocity of the mechanical system to the forces.
5. The contacts of the mechanical system on position level remain unchanged in their status, such that the set $\mathcal{I}_\mathrm{S}$ remains unchanged.

Definition Hybrid Executions of switching Lagrangian Systems A hybrid execution also called a hybrid trajectory of a switching Lagrangian system defined on a time interval $[t_0,\, t_\mathrm{f}]$ if there is a finite partition of $[t_0,\, t_\mathrm{f}]$, $\mathcal{P} = t_0 \leq t_1, \ldots, t_{p+1} = t_\mathrm{f}$, $p \geq 0$, and a succession of discrete modes $\{a_0, \ldots, a_p\} \in \mathcal{I}_M$ and arcs $\pi_0, \ldots, \pi_m$, such that

1. $(a_\mathrm{j}, a_{\mathrm{j}+1}) \in \mathcal{E}_\mathrm{T}$ for $j = 0, \ldots, p-1$;
2. $a_\mathrm{j} : [t_\mathrm{j}, t_{\mathrm{j}+1}] \to \mathcal{M}_{l_\mathrm{j}}$ is a continuous and piecewise $\mathcal{C}^\infty$ curve in $\mathcal{M}_{l_\mathrm{j}}$ for $j = 0, \ldots p$;

There are many classes of switching hybrid dynamical systems and based on this diversity many optimal control approaches have been developed and investigated. The complexity of such problems poses challenges both theoretically and numerically. In two publications [Xu and Antsaklis, 2002a] and [Xu and Antsaklis, 2002b] present Xu and Antsaklis a direct numerical method for the switching time optimization for systems without state discontinuity at transitions based on numerical and analytical differentiations of the value function. The issue of differentiability and continuity of the value function is a complex one, and requires the pre-specification of the mode sequence and partitioning of the considered hybrid optimal control problem in advance. Egerstedt *et. al.* discuss in [Egerstedt, Wardi and Axelsson, 2006] and [Egerstedt, Wardi

and Delmotte, 2003] a numerical algorithm based on the calculation of the gradient of the value function w.r.t to switching times and propose a gradient descent based algorithm that determines suboptimal solutions. The major difference between this work and the cited works in literature, is that the mechanical dynamics is represented as a measure-differential inclusion. By the validity of the measure-differential inclusion representation at even instants of discontinuity and the intrinsic property that set-valued force laws and set-valued control laws are incorporated in the dynamics straightforward, enables that for certain classes of mechanical systems every instant becomes a potential transition time. A novel work dedicated to the treatment of set-valued force laws is given in [Glocker, 2001].

1 Modeling of Switching Lagrangian Systems

Let $\mathbf{q}, \dot{\mathbf{q}}, \ddot{\mathbf{q}}$ represent the position, velocity and acceleration in the generalised coordinates of a scleronomic finite-dimensional Lagrangian system with n maximal degrees of freedom (DOF), respectively. The tangential and normal local kinematics need to be defined in order to relate the contact distance to the set-valued force element. For the detection of the closing of a contact let the $m \times 1$ vector $\mathbf{g}(\mathbf{q})$ denote the normal contact distances between the rigid bodies in the system which are always non-negative due to the impenetrability assumption. The normal and tangential contact velocities $\boldsymbol{\gamma}_\mathrm{u}$,$\boldsymbol{\gamma}_\mathrm{s} \in \mathbb{R}^\mathrm{m}$ are defined as:

$$\boldsymbol{\gamma}_\mathrm{u} = \mathbf{D}_\mathrm{u}^\mathrm{T}\dot{\mathbf{q}} \quad \text{and} \quad \boldsymbol{\gamma}_\mathrm{s} = \mathbf{D}_\mathrm{s}^\mathrm{T}\dot{\mathbf{q}}, \tag{1}$$

respectively, and $\boldsymbol{\gamma}_\mathrm{u}$ is obtained as the total time derivative of $\mathbf{g}(\mathbf{q})$. The normal and tangential contact accelerations are given as in equation (2):

$$\dot{\boldsymbol{\gamma}}_\mathrm{u} = \mathbf{D}_\mathrm{u}^\mathrm{T}\ddot{\mathbf{q}} + \boldsymbol{\omega}_\mathrm{u}, \quad \dot{\boldsymbol{\gamma}}_\mathrm{s} = \mathbf{D}_\mathrm{s}^\mathrm{T}\ddot{\mathbf{q}} + \boldsymbol{\omega}_\mathrm{s}. \tag{2}$$

The contact forces, which are non-potential in the classical sense, are incorporated by the appropriate generalised force directions $\mathbf{D}_\mathrm{s}$ and $\mathbf{D}_\mathrm{u}$ in the equations of motion. In order to formulate the contact situations properly following index sets are defined:

$$\mathcal{I}_\mathrm{G} = \{1, 2, ...p\}, \tag{3}$$
$$\mathcal{I}_\mathrm{S} = \{i \in \mathcal{I}_\mathrm{G} |\, g_{\mathrm{u}_\mathrm{i}} = 0\}, \tag{4}$$
$$\mathcal{I}_\mathrm{U} = \{i \in \mathcal{I}_\mathrm{G} |\, g_{\mathrm{u}_\mathrm{i}} = 0,\, \boldsymbol{\gamma}_{\mathrm{u}_\mathrm{i}} = 0\}. \tag{5}$$

$\mathcal{I}_\mathrm{G}$ denotes the set of all contacts that can occur on position level of the non-smooth mechanical system and the total number amounts to p. $\mathcal{I}_\mathrm{S}$ denotes the set of all contacts that are closed on position level of the system and the total number amounts to m. $\mathcal{I}_\mathrm{U}$ denotes the set of all contacts with r elements so that normal contact velocity and normal contact distance equal to zero. Further, the definition of following index sets are necessary:

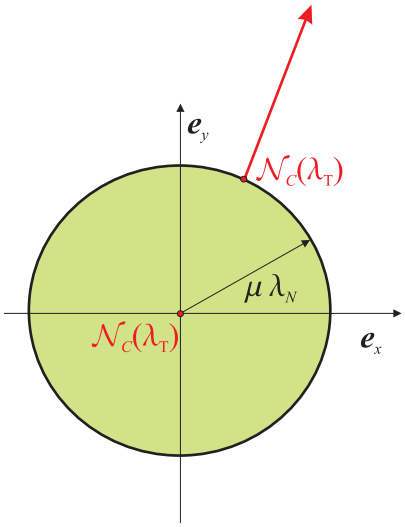

Figure 1. The spatial frictional disc with normal force dependent radius and various normal cones.

$$\mathcal{C}_{\mathrm{u}_\mathrm{i}} = \{\lambda_{\mathrm{u}_\mathrm{i}} \,|\, \lambda_{\mathrm{u}_\mathrm{i}} \geq 0, \quad \forall\, i \in \mathcal{I}_\mathrm{G}\}, \tag{6}$$
$$\mathcal{C}_{\mathrm{s}_\mathrm{i}}(\lambda_{\mathrm{u}_\mathrm{i}}) = \{\boldsymbol{\lambda}_{\mathrm{s}_\mathrm{i}} \,|\quad |\boldsymbol{\lambda}_{\mathrm{s}_\mathrm{i}}| \leq \mu_\mathrm{i}\,\lambda_{\mathrm{u}_\mathrm{i}}, \quad \forall\, i \in \mathcal{I}_\mathrm{S}\}, \tag{7}$$

where the vectors $\boldsymbol{\lambda}_\mathrm{s}, \boldsymbol{\lambda}_\mathrm{u}$ are the tangential and the normal contact forces, respectively and μ_i denotes the friction coefficient at contact i. The differential inclusion of a general non-autonomous mechanical system subject to spatial friction and unilateral contact forces in the absence of impacts is stated as:

$$\begin{aligned}&\mathbf{M}(\mathbf{q})\,\ddot{\mathbf{q}} - \mathbf{h}(\mathbf{q},\,\dot{\mathbf{q}}) && (8)\\ &\qquad -\mathbf{D}_\mathrm{s}(\mathbf{q})\boldsymbol{\lambda}_\mathrm{s} - \mathbf{D}_\mathrm{u}(\mathbf{q})\boldsymbol{\lambda}_\mathrm{u} - \mathbf{B}(\mathbf{q})\,\boldsymbol{\tau} = \mathbf{0}, \quad \text{a.e.}\\ &-\dot{\gamma}_{\mathrm{u}_\mathrm{i}} \in \mathcal{N}_{\mathcal{C}_{\mathrm{u}_\mathrm{i}}}(\lambda_{\mathrm{u}_\mathrm{i}}), \quad \forall\, i \in \mathcal{I}_\mathrm{U}, && (9)\\ &-\dot{\boldsymbol{\gamma}}_{\mathrm{s}_\mathrm{i}} \in \mathcal{N}_{\mathcal{C}_{\mathrm{s}_\mathrm{i}}(\lambda_{\mathrm{u}_\mathrm{i}})}(\boldsymbol{\lambda}_{\mathrm{s}_\mathrm{i}}), \quad \forall\, i \in \mathcal{I}_\mathrm{U}. && (10)\end{aligned}$$

$\mathbf{M}(\mathbf{q})$ is the symmetric positive-definite (PD) mass matrix and $\mathbf{h}(\mathbf{q},\,\dot{\mathbf{q}})$ represents the vector with gyroscopic, centripedal and coriolis accelerations along with smooth force laws such as springs and dampers, $\mathbf{B}(\mathbf{q})$ is the generalised force direction of controls. The vector $\boldsymbol{\tau} \in \mathbb{R}^\mathrm{s}$ denotes the vector of control inputs. The normal cone to a set C at the point $\mathbf{x} \in \mathcal{C}$ is given by $\mathcal{N}_\mathrm{C}(\mathbf{x})$. If a spatial mechanical system with n degrees of freedom having contacts with spatial friction is considered, then $\mathbf{D}_\mathrm{s}(\mathbf{q})$ is a $n \times r$ linear operator of generalised friction force directions; $\mathbf{D}_\mathrm{u}(\mathbf{q})$ is a $n \times r$ linear operator of generalised normal force directions. For systems where normal contact forces are passive forces, the normal forces can be determined by the projection of the change of linear and angular momenta in

the constrained directions

$$\boldsymbol{\lambda}_{\mathrm{u}} = \mathbf{P}_{\mathrm{a}}\left(\mathbf{q},\, \dot{\mathbf{q}},\, \ddot{\mathbf{q}},\, \boldsymbol{\tau},\, \boldsymbol{\lambda}_{\mathrm{s}}\right) = \mathbf{V}_{\mathrm{a}}(\mathbf{q},\, \dot{\mathbf{q}},\, \ddot{\mathbf{q}}) + \mathbf{R}_{\mathrm{a}}(\mathbf{q})\,\boldsymbol{\lambda}_{\mathrm{s}} + \mathbf{S}_{\mathrm{a}}(\mathbf{q})\,\boldsymbol{\tau}, \tag{11}$$

where $\mathbf{P}_{\mathrm{a}}$ is a set of algebraic equations which are explicitly solved for the normal contact forces, where $\mathbf{S}_{\mathrm{a}}(\mathbf{q})$ and $\mathbf{R}_{\mathrm{a}}(\mathbf{q})$ are $p \times s$ and $p \times p$ dimensional linear operators respectively. Since no adhesive forces at contacts are allowed, the normal contact forces that are obtained by the projection have to be restrained to $\mathbb{R}_0^+$. The differential inclusion in (8) becomes:

$$\mathbf{M}(\mathbf{q})\,\ddot{\mathbf{q}} - \mathbf{h}(\mathbf{q},\, \dot{\mathbf{q}}) - \mathbf{D}_{\mathrm{s}}(\mathbf{q})\boldsymbol{\lambda}_{\mathrm{s}} - \mathbf{B}(\mathbf{q})\,\boldsymbol{\tau} = \mathbf{0}, \tag{12}$$

$$\boldsymbol{\lambda}_{\mathrm{u}} = \mathrm{proj}_{\mathbb{R}_0^+}\left(\mathbf{P}_{\mathrm{a}}\left(\mathbf{q},\, \dot{\mathbf{q}},\, \ddot{\mathbf{q}},\, \boldsymbol{\tau},\, \boldsymbol{\lambda}_{\mathrm{s}}\right)\right),\, \forall\, i \in \mathcal{I}_{\mathrm{U}}, \tag{13}$$

$$-\,\dot{\boldsymbol{\gamma}}_{\mathrm{s_i}} \in \mathcal{N}_{\mathcal{C}_{\mathrm{s_i}}(\lambda_{\mathrm{u_i}})}\left(\boldsymbol{\lambda}_{\mathrm{s_i}}\right),\, \forall\, i \in \mathcal{I}_{\mathrm{U}}. \tag{14}$$

The dynamics of a mechanical System can be formulated on the measure-differential level by considering the dynamic balance as an equality of measures:

$$\mathbf{M}(\mathbf{q})\,d\dot{\mathbf{q}} - \mathbf{h}(\mathbf{q},\, \dot{\mathbf{q}}^+)\,dt - \mathbf{D}_{\mathrm{s}}(\mathbf{q})\,d\boldsymbol{\Lambda}_{\mathrm{s}} - \mathbf{D}_{\mathrm{u}}(\mathbf{q})\,d\boldsymbol{\Lambda}_{\mathrm{u}} - \mathbf{B}(\mathbf{q})\,\boldsymbol{\tau}\,dt = \mathbf{0}, \tag{15}$$

$$-\,\gamma_{\mathrm{u_i}}^+ \in \mathcal{N}_{\mathcal{C}_{\mathrm{u_i}}}(d\Lambda_{\mathrm{u_i}}), \quad \forall\, i \in \mathcal{I}_{\mathrm{S}}, \tag{16}$$

$$-\,\boldsymbol{\gamma}_{\mathrm{s_i}}^+ \in \mathcal{N}_{\mathcal{C}_{\mathrm{s_i}}(d\Lambda_{\mathrm{u_i}})}(d\boldsymbol{\Lambda}_{\mathrm{s_i}}), \quad \forall\, i \in \mathcal{I}_{\mathrm{S}}. \tag{17}$$

Here $d\boldsymbol{\Lambda}_{\mathrm{s}}$ and $d\boldsymbol{\Lambda}_{\mathrm{u}}$ are the differential measures of the tangential and normal contact forces, respectively and $d\dot{\mathbf{q}}$ denotes the differential measure of the generalised velocity. An exposition of measure differential inclusions in control form can be found in [Yunt, 2007a]. Similarly, by the projection of the differential measures of angular and linear momenta, equations of the form as given in equation (18) can be obtained:

$$d\boldsymbol{\Lambda}_{\mathrm{u}} = \mathbf{P}_{\mathrm{v}}\left(\mathbf{q},\, \dot{\mathbf{q}}^+,\, d\dot{\mathbf{q}},\, \boldsymbol{\tau},\, d\boldsymbol{\Lambda}_{\mathrm{s}}, dt\right) = \mathbf{V}_{\mathrm{v}}(\mathbf{q},\, \dot{\mathbf{q}}^+,\, d\dot{\mathbf{q}}) + R_{\mathrm{v}}(\mathbf{q})\; d\boldsymbol{\Lambda}_{\mathrm{s}} + S_{\mathrm{v}}(\mathbf{q})\,\boldsymbol{\tau}\,dt, \tag{18}$$

where $\mathbf{P}_{\mathrm{v}}$ is a set of algebraic equations which are explicitly solved for the normal contact forces, where $\mathbf{S}_{\mathrm{v}}(\mathbf{q})$ and $\mathbf{R}_{\mathrm{v}}(\mathbf{q})$ are $m \times s$ and $m \times m$ dimensional linear operators respectively. Since no adhesive forces at contacts are allowed, the normal contact forces that are obtained by the projection have to be restrained to $\mathbb{R}_0^+$. Similarly, the equations (15), (16), (17) converts into:

$$\begin{aligned}
\mathbf{M}\,d\dot{\mathbf{q}} &- \mathbf{D}_{\mathrm{s}}(\mathbf{q})\; d\boldsymbol{\Lambda}_{\mathrm{s}} \\
&- \left(\mathbf{h}(\mathbf{q},\, \dot{\mathbf{q}}^+) + \mathbf{B}(\mathbf{q})\,\boldsymbol{\tau}\right)\, dt = \mathbf{0}, && (19)\\
d\boldsymbol{\Lambda}_{\mathrm{u}} &= \mathrm{proj}_{\mathbb{R}_0^+}\left(\mathbf{P}_{\mathrm{v}}\left(\mathbf{q},\, \dot{\mathbf{q}}^+,\, d\dot{\mathbf{q}},\, \boldsymbol{\tau},\; d\boldsymbol{\Lambda}_{\mathrm{s}}, dt\right)\right), \\
&\qquad \forall\, i \in \mathcal{I}_{\mathrm{S}}, && (20)\\
-\boldsymbol{\gamma}_{\mathrm{s_i}}^+ &\in N_{\mathcal{C}_{\mathrm{s_i}}(d\Lambda_{\mathrm{u_i}})}\left(d\boldsymbol{\Lambda}_{\mathrm{s_i}}\right), \quad \forall\, i \in \mathcal{I}_{\mathrm{S}}. && (21)
\end{aligned}$$

By passing from the representation from acceleration level as in (12) to measure-differential level as in (19) the contact index sets has changed form $\mathcal{I}_{\mathrm{U}}$ to $\mathcal{I}_{\mathrm{S}}$ so in the numerical evaluations the need to distinguish between positive relative contact velocities and zero contact velocities has been removed and all closed contacts are considered.

2 Treatment of Contact Dynamics and Time-Stepping Integration

The normal cone representation in contact mechanics and friction problems are first treated in [Moreau, 1988] and [Alart and Curnier, 1991], respectively. The above relation enables the reformulation of the set-valued relation given in (19) in an equality form:

$$\begin{aligned}
\mathbf{M}\,d\dot{\mathbf{q}} &- \mathbf{D}_{\mathrm{s}}(\mathbf{q})\; d\boldsymbol{\Lambda}_{\mathrm{s}} \\
&- \left(\mathbf{h}(\mathbf{q},\, \dot{\mathbf{q}}^+) + \mathbf{B}(\mathbf{q})\,\boldsymbol{\tau}\right)\, dt = \mathbf{0}, && (22)\\
& && (23)\\
d\boldsymbol{\Lambda}_{\mathrm{u}} &= \mathrm{proj}_{\mathbb{R}_0^+}\left(\mathbf{P}_{\mathrm{v}}\left(\mathbf{q},\, \dot{\mathbf{q}}^+,\, d\dot{\mathbf{q}},\, \boldsymbol{\tau},\; d\boldsymbol{\Lambda}_{\mathrm{s}}, dt\right)\right), \\
&\qquad \forall\, i \in \mathcal{I}_{\mathrm{S}}, && (24)\\
d\boldsymbol{\Lambda}_{\mathrm{s_i}} &= \mathrm{proj}_{\mathcal{C}_{\mathrm{s_i}}(d\Lambda_{\mathrm{u_i}})}\left(d\boldsymbol{\Lambda}_{\mathrm{s_i}} - r\,\boldsymbol{\gamma}_{\mathrm{s_i}}^+\right), \quad \forall i \in \mathcal{I}_{\mathrm{S}}. && (25)
\end{aligned}$$

To perform numerical integration of a system with respect to time, one has to address the following problem: For given initial time t^{j} and known initial displacements $\mathbf{q}(t^{\mathrm{j}}) = \mathbf{q}^{\mathrm{j}} \in \mathbb{R}^{\mathrm{n}}$ and velocities $\dot{\mathbf{q}}^{\mathrm{j}} = \dot{\mathbf{q}}(t^{\mathrm{j}}) \in \mathbb{R}^{\mathrm{n}}$, find approximations of the displacements $\mathbf{q}(t^{\mathrm{j}}) = \mathbf{q}^{\mathrm{j}} \in \mathbb{R}^{\mathrm{n}}$ and velocities $\dot{\mathbf{q}}^{\mathrm{j}} = \dot{\mathbf{q}}(t^{\mathrm{j}}) \in \mathbb{R}^{\mathrm{n}}$ at the end $t^{\mathrm{j+1}}$ of a chosen time interval $[t^{\mathrm{j}}, t^{\mathrm{j+1}}]$. To apply the midpoint rule, the following steps have to be performed.

1. Given a time step $t^{\mathrm{j}} + \Delta\, t = t^{\mathrm{j+1}}$,compute the midpoint $t^{\mathrm{m}} = t^{\mathrm{j}} + \frac{1}{2}\,\Delta t$ and the endpoint $t^{\mathrm{j+1}} = t^{\mathrm{j}} + \Delta t$ of the time interval.
2. Approximate midpoint displacements by $\mathbf{q}^{\mathrm{m}} = \mathbf{q}^{\mathrm{j}} + \frac{1}{2}\Delta t \cdot \dot{\mathbf{q}}^{\mathrm{j}} \in \mathbb{R}^{\mathrm{n}}$
3. Matrix calculations:
   Compute $\mathbf{M}(\mathbf{q}^{\mathrm{m}}) \in \mathbb{R}^{n \times n}$ and $\mathbf{h}(\mathbf{q}^{\mathrm{m}}, \dot{\mathbf{q}}^{\mathrm{j}}) \in \mathbb{R}^{\mathrm{n}}$
   For $i = 1, \ldots p$ set up the index set $\mathcal{I}_{\mathrm{S}} = \{i | g_{\mathrm{u_i}}(\mathbf{q}^{\mathrm{m}}, t^{\mathrm{m}}) \leq 0\}$.
   For every $i \in \mathcal{I}_{\mathrm{S}}$ compute $\mathbf{d}_{\mathrm{s_i}}(\mathbf{q}^{\mathrm{m}}) \in \mathbb{R}^{1 \times n}$ and $\omega_{\mathrm{s_i}}(\mathbf{q}^{\mathrm{m}}) \in \mathbb{R}^{1 \times n}$.
4. Determination of $\dot{\mathbf{q}}^{\mathrm{j+1}}$: In this step following equations have to be solved:

$$\begin{aligned}
&\mathbf{M}(\dot{\mathbf{q}}^{\mathrm{j+1}} - \dot{\mathbf{q}}^{\mathrm{j}}) && (26)\\
&-\mathbf{h}\,\Delta\, t - \mathbf{D}_{\mathrm{s_i}}^{\mathrm{T}}\,\Lambda_{\mathrm{s_i}} - \mathbf{B}(\mathbf{q}^{\mathrm{m}})\boldsymbol{\tau}^{\mathrm{l(i)}}\Delta\, t = \mathbf{0} \\
&\gamma_{\mathrm{s_i}}^{\mathrm{j+1}} = \mathbf{D}_{\mathrm{s_i}}^{\mathrm{T}}\,\dot{\mathbf{q}}^{\mathrm{j+1}} + \boldsymbol{\omega}_{\mathrm{s_i}}\left(\mathbf{q}^{\mathrm{m}}\right) && (27)\\
&\boldsymbol{\Lambda}_{\mathrm{u}} = && (28)\\
&\mathrm{proj}_{\mathbb{R}_0^+}\left(\mathbf{P}_{\mathrm{v}}\left(\mathbf{q}^{\mathrm{m}},\, \dot{\mathbf{q}}^{\mathrm{j+1}} - \dot{\mathbf{q}}^{\mathrm{j}}, \boldsymbol{\tau}^{\mathrm{l(i)}},\; \boldsymbol{\Lambda}_{\mathrm{s}}, \Delta\, t\right)\right), \\
&\Lambda_{\mathrm{s_i}} = \mathrm{proj}_{\mathcal{C}_{\mathrm{s_i}}(\Lambda_{\mathrm{u_i}})}\left(\Lambda_{\mathrm{s_i}} - r\,\gamma_{\mathrm{s_i}}^{\mathrm{j+1}}\right), \quad \forall i \in \mathcal{I}_{\mathrm{S}}.
\end{aligned}$$

5. Computation $\mathbf{q}^{\mathrm{j}+1} = \mathbf{q}^{\mathrm{m}} + \frac{1}{2}\Delta t \cdot \dot{\mathbf{q}}^{\mathrm{j}+1} \in \mathbb{R}^{\mathrm{n}}$

The vectors $\mathbf{\Lambda}_{\mathrm{s}}$ and $\mathbf{\Lambda}_{\mathrm{u}}$ represent the discretised form of the tangential and normal contact differential measures, that exist in a distributional sense on the interval $[t^{\mathrm{j}}, t^{\mathrm{j}+1}]$. The solution of step 4 for is accomplished iteratively:

$$
\begin{aligned}
&\dot{\mathbf{q}}_{\mathrm{k}+1}^{\mathrm{j}+1} = \dot{\mathbf{q}}^{\mathrm{j}} - \mathbf{M}^{-1}(\mathbf{q}^{\mathrm{m}})\mathbf{h}(\mathbf{q}^{\mathrm{m}}, \dot{\mathbf{q}}^{\mathrm{j}})\,\Delta t \\
&+ \mathbf{M}^{-1}(\mathbf{q}^{\mathrm{m}}) \left(\mathbf{D}_{\mathrm{s_i}}(\mathbf{q}^{\mathrm{m}})\,\Lambda_{\mathrm{s_i}}^{\mathrm{k}} + \mathbf{B}(\mathbf{q}^{\mathrm{m}})\boldsymbol{\tau}^{\mathrm{l(i)}}\Delta t \right), \\
&{}_{\mathrm{k}+1}\gamma_{\mathrm{s_i}}^{\mathrm{j}+1} = \mathbf{D}_{\mathrm{s_i}}{}^{\mathrm{T}}\,\dot{\mathbf{q}}_{\mathrm{k}+1}^{\mathrm{j}+1} + \boldsymbol{\omega}_{\mathrm{s_i}}(\mathbf{q}^{\mathrm{m}}), \\
&\mathbf{\Lambda}_{\mathrm{u}}^{\mathrm{k}+1} = \\
&\mathrm{proj}_{\mathbb{R}_0^+} \left(\mathbf{P}_{\mathrm{v}} \left(\mathbf{q}^{\mathrm{m}},\, \dot{\mathbf{q}}_{\mathrm{k}}^{\mathrm{j}+1} - \dot{\mathbf{q}}^{\mathrm{j}}, \boldsymbol{\tau}^{\mathrm{l(i)}},\, \mathbf{\Lambda}_{\mathrm{s}}^{\mathrm{k}+1}, \Delta t \right) \right), \\
&\Lambda_{\mathrm{s_i}}^{\mathrm{k}+1} = \mathrm{proj}_{\mathcal{C}_{\mathrm{s_i}}(\Lambda_{\mathrm{u_i}}^{\mathrm{k}})} \left(\Lambda_{\mathrm{s_i}}^{\mathrm{k}} - r\ {}_{\mathrm{k}+1}\gamma_{\mathrm{s_i}}^{\mathrm{j}+1} \right), \quad \forall i \in \mathcal{I}_{\mathrm{S}}.
\end{aligned}
$$

At each integration time point, the embedded iterations are stopped when the norm of change of successive discretised normal and tangential contact force measures $\|\Lambda_{\mathrm{s_i}}^{\mathrm{k}+1} - \Lambda_{\mathrm{s_i}}^{\mathrm{k}}\|$ and $\|\Lambda_{\mathrm{u_i}}^{\mathrm{k}+1} - \Lambda_{\mathrm{u_i}}^{\mathrm{k}}\|$ is less than a specified tolerance. More advanced discretisation schemes may be found in the literature, such as the powerful Θ-method, an algorithm based on displacements with proven convergence. The literature on the time-stepping based simulation of systems with friction is vast and a good overview is provided in [Anitescu and Florian, 2001], [Stewart and Trinkle, 1996], [Studer and Glocker, 2006], [Studer and Glocker, 2007].

2.1 Formulation of the Trajectory Optimisation of Mechanical Systems

In references [Rockafellar, 1976], [Rockafellar, 1974] and [Rockafellar, 1981] an overview on the properties and the need for the development of augmented Lagrangian approach. Consider a general switching finite-dimensional Lagrangian system described by equation (19) having n general coordinates. Let the controls be discretised by N_c points and the positions and velocities be discretised by N_{s} where the time-stepping integration defines a nonlinear discrete single-valued mapping $\mathcal{I} : \mathbb{R}^{2\,n+m\,N_c+1} \rightarrow \mathbb{R}^{2\,\mathrm{n}}$, that relates the final position $\mathbf{q}_{\mathrm{f}}$ and velocity $\dot{\mathbf{q}}_{\mathrm{f}}$ to the initial position $\mathbf{q}_0$, initial velocity $\dot{\mathbf{q}}_0$ and the primal variables of optimisation $\mathbf{y}^{\mathrm{k}}$ as follows:

$$
\begin{pmatrix} \mathbf{q}_{\mathrm{f}} \\ \dot{\mathbf{q}}_{\mathrm{f}} \end{pmatrix} = \mathcal{I}(\mathbf{y}, \mathbf{q}_0, \dot{\mathbf{q}}_0). \tag{29}
$$

Here $\mathbf{y}$ is composed of the actuating torques/forces end the final time $\mathbf{y} = (\boldsymbol{\tau}\,, t_{\mathrm{f}}) \in \mathbb{R}^{m\,N_c+1}$. Furthermore let the final desired state be specified by a set of equalities/inequalities and constraints be imposed on the controls as well as the end state as follows:

$$
\mathcal{C} = \left\{ \mathbf{y} | \begin{pmatrix} \boldsymbol{\tau}_{\min} \\ t_{\mathrm{fmin}} \end{pmatrix} \leq \begin{pmatrix} \boldsymbol{\tau} \\ t_{\mathrm{f}} \end{pmatrix} \leq \begin{pmatrix} \boldsymbol{\tau}_{\max} \\ t_{\mathrm{fmax}} \end{pmatrix} \right\}, \tag{30}
$$

and let the fulfillment of the following set of equalities suffice for the reaching of the final state:

$$
\mathbf{\Delta}_{\mathrm{f}} = \begin{pmatrix} \mathbf{q}_{\mathrm{f}} - \mathbf{q}_{\mathrm{d}} \\ \dot{\mathbf{q}}_{\mathrm{f}} - \dot{\mathbf{q}}_{\mathrm{d}} \end{pmatrix} = \mathbf{0} \in \mathbb{R}^{2\,\mathrm{N}}. \tag{31}
$$

Here $\mathbf{q}_d$ and $\dot{\mathbf{q}}_d$ represent the desired end position and velocity of the mechanical system, respectively. Then the successive minimisation of the following augmented Lagrangian function yields an at least locally optimal trajectory if a feasible set exists:

$$
\begin{aligned}
&\min_{\mathbf{y}}\ L_{\mathrm{a}}(\mathbf{y}, \boldsymbol{\nu}^{\mathrm{k}}, \boldsymbol{\mu}^{\mathrm{k}}) = f(\mathbf{y}) + \left\langle \boldsymbol{\mu}^{\mathrm{k}}, \mathbf{\Delta}_{\mathrm{f}} \right\rangle \qquad (32) \\
&+ \frac{c^{\mathrm{k}}}{2} \left\langle \mathbf{\Delta}_{\mathrm{f}}\,, \mathbf{\Delta}_{\mathrm{f}} \right\rangle + \frac{1}{2\,c^{\mathrm{k}}} \left(\left\langle \boldsymbol{\nu}^{\mathrm{k}+1}\,, \boldsymbol{\nu}^{\mathrm{k}+1} \right\rangle - \left\langle \boldsymbol{\nu}^{\mathrm{k}},\, \boldsymbol{\nu}^{\mathrm{k}} \right\rangle \right)
\end{aligned}
$$

where $\boldsymbol{\nu}^{\mathrm{k}+1}$ and $\boldsymbol{\mu}^{\mathrm{k}+1}$ are given by:

$$
\boldsymbol{\nu}^{\mathrm{k}+1} = proj_{\mathbb{R}_0^+} \left(\boldsymbol{\nu}^{\mathrm{k}} + c^{\mathrm{k}}\,\mathbf{g}(\mathbf{y}^{\mathrm{k}}) \right), \tag{33}
$$

$$
\boldsymbol{\mu}^{\mathrm{k}+1} = \boldsymbol{\mu}^{\mathrm{k}} + c^{\mathrm{k}}\,\mathbf{h}(\mathbf{y}^{\mathrm{k}}). \tag{34}
$$

Here $\mathbf{y}^{\mathrm{k}}$ is given by:

$$
\mathbf{y}^{\mathrm{k}} = \arg\min_{\mathbf{y}}\ L_{\mathrm{a}}(\mathbf{y}, \boldsymbol{\nu}^{\mathrm{k}}, \boldsymbol{\mu}^{\mathrm{k}}). \tag{35}
$$

Here $\boldsymbol{\mu} \in \mathbb{R}^{2\,\mathrm{n}}$ and $\boldsymbol{\nu} \in \mathbb{R}^{2\,m\,N_c+2}$ denote the Lagrange multiplier vectors belonging to the equality and inequality constraint vectors, and $\mathbf{g}(\mathbf{y})$ the inequalities imposed on the controls and end time given by the set $\mathcal{C}$. The successive minimisations of the augmented Lagrangian $L_{\mathrm{a}}(\mathbf{y}^{\mathrm{k}}, \boldsymbol{\nu}^{\mathrm{k}}, \boldsymbol{\mu}^{\mathrm{k}})$ as $c_{\mathrm{k}} \rightarrow +\infty$ and $c_{\mathrm{k}+1} > c_{\mathrm{k}}$ is assured to reveal a global or a local minimum if a nonempty solution set exists. The Nelder-Mead simplex method is used to perform the successive minimisations of $L_{\mathrm{a}}(\mathbf{y}, \boldsymbol{\nu}^{\mathrm{k}}, \boldsymbol{\mu}^{\mathrm{k}})$ with respect to $\mathbf{y}$, which is a non-gradient based minimisation algorithm, that performs the minimisations based on a function value comparison strategy.

3 Numerical Results

The model has first been introduced in [Yunt and Glocker, 2005] and in [Yunt, 2006] the convergence proof and the optimality certificate for the optimal trajectories are given. In the Appendix the parameters used for the optimization and linear operators $\mathbf{M}$, $\mathbf{h}$ and $\mathbf{B}$ that characterize the equations of motion are given. The differential-drive robot is a three-wheeled actuated robot of which the rear wheels are actuated and controlled separately contrary to the front wheel which is neither actuated nor steered. A rigid-body mechanical model is used, in which the friction between wheels and ground is modeled as isotropic spatial Coulomb friction. The non-steered unactuated front wheel is replaced by a stick as a simplification, removing two degrees of freedom (DOF) to be modeled. The rotational

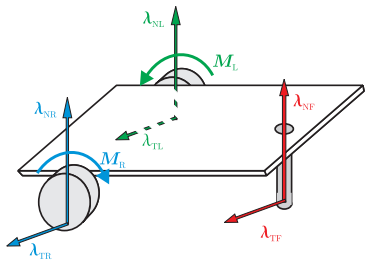

Figure 2. Contact forces and motor moments on the simplified model.

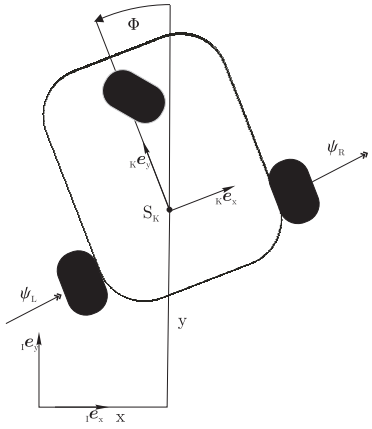

Figure 3. The generalized coordinates of the wheeled robot.

inertia of the total actuation consisting of the components of motor rotors and transmissions are added to the rotational inertias of the wheels. The resulting mass matrix of the differential-drive robot has the following sparse structure:

$$M = \begin{bmatrix} m_{11} & 0 & m_{13} & 0 & 0 \\ 0 & m_{22} & m_{23} & 0 & 0 \\ m_{31} & m_{32} & m_{33} & 0 & 0 \\ 0 & 0 & 0 & m_{44} & 0 \\ 0 & 0 & 0 & 0 & m_{55} \end{bmatrix}. \qquad (36)$$

The entries of the symmetric positive-definite mass matrix are given by:

$$\begin{aligned} & m_{11} = m_{22} = m_{\mathrm{R}} + m_{\mathrm{L}} + m_{\mathrm{K}}, \\ & m_{13} = m_{31} = -m_{\mathrm{L}} \sin(\phi) l_{\mathrm{x}} \\ & -m_{\mathrm{R}} \cos(\phi) r_{\mathrm{y}} - m_{\mathrm{R}} \sin(\phi)\, r_{\mathrm{x}} - m_{\mathrm{L}} \cos(\phi) l_{\mathrm{y}}, \\ & m_{33} = \\ & 2\,b + k_{33} + m_{\mathrm{R}}\, {r_{\mathrm{x}}}^2 + m_{\mathrm{R}}\, {r_{\mathrm{y}}}^2 + m_{\mathrm{L}}\, {l_{\mathrm{x}}}^2 + m_{\mathrm{L}}\, {l_{\mathrm{y}}}^2, \\ & m_{23} = m_{32} = -m_{\mathrm{L}} \sin(\phi) l_{\mathrm{y}} \\ & + m_{\mathrm{L}} \cos(\phi) l_{\mathrm{x}} + m_{\mathrm{R}} \cos(\phi) r_{\mathrm{x}} - m_{\mathrm{R}} \sin(\phi)\, r_{\mathrm{y}}, \\ & m_{44} = m_{55} = a. \end{aligned}$$

The vector of gyroscopic and coriolis forces $\mathbf{h}$ does not contain any coupling between the actuated and nonactuated degrees of freedom.The vector $\mathbf{h}$ is given by the following expression:

$$\mathbf{h} = \left[-\dot{\phi}^2 v \;\; \dot{\phi}^2 w \;\; 0 \;\; M_{\mathrm{L}} \;\; -M_{\mathrm{R}} \right]^{\mathrm{T}}. \qquad (37)$$

The terms v and w are given by:

$$\begin{aligned} v &= m_{\mathrm{R}} \sin(\phi)\, r_{\mathrm{y}} - m_{\mathrm{R}} \cos(\phi)\, r_{\mathrm{x}} \\ &\quad + m_{\mathrm{L}} \sin(\phi)\, l_{\mathrm{y}} - m_{\mathrm{L}} \cos(\phi)\, l_{\mathrm{x}}, \\ w &= m_{\mathrm{L}} \cos(\phi)\, l_{\mathrm{y}} + m_{\mathrm{L}} \sin(\phi)\, l_{\mathrm{x}} \\ &\quad + m_{\mathrm{R}} \cos(\phi)\, r_{\mathrm{y}} + m_{\mathrm{R}} \sin(\phi)\, r_{\mathrm{x}}. \end{aligned}$$

The mechanical system has four modes of operation, and their are classified according to the contact relative velocities ${}_{\mathrm{K}}\boldsymbol{\gamma}_{\mathrm{R}} = {}_{\mathrm{K}}D_{\mathrm{CR}}^{\mathrm{T}}\dot{\mathbf{q}}$ and ${}_{\mathrm{K}}\boldsymbol{\gamma}_{\mathrm{l}} = {}_{\mathrm{K}}D_{\mathrm{CL}}^{\mathrm{T}}\dot{\mathbf{q}}$ in table (1). The linear operator of generalised friction force and generalised control force directions are given by:

$${}_{\mathrm{K}}D_{\mathrm{CR}}^{\mathrm{T}} = \begin{bmatrix} \cos(\phi) & \sin(\phi) & -r_{\mathrm{y}} & 0 & 0 \\ -\sin(\phi) & \cos(\phi) & r_{\mathrm{x}} & 0 & r \\ 0 & 0 & 0 & 0 & 0 \end{bmatrix},$$

$${}_{\mathrm{K}}D_{\mathrm{CL}}^{\mathrm{T}} = \begin{bmatrix} \cos(\phi) & \sin(\phi) & -l_{\mathrm{y}} & 0 & 0 \\ -\sin(\phi) & \cos(\phi) & l_{\mathrm{x}} & r & 0 \\ 0 & 0 & 0 & 0 & 0 \end{bmatrix},$$

$$\mathbf{B} = \begin{bmatrix} 0 & 0 \\ 0 & 0 \\ 0 & 0 \\ 0 & 1 \\ -1 & 0 \end{bmatrix},$$

respectively. When the nonholonomic constraints and rolling constraints are fulfilled, the non-actuated mechanical system possesses two DOF. If both wheels slide it is a mechanical system with five DOF. In the three-DOF mode one wheel contact sticks and the other wheel slides, meaning that the nonholonomic constraints are fulfilled but one wheel does not fulfill the rolling condition. Because of the geometry of the wheels, in the 2-DOF and 3-DOF mode the transversal components of the friction forces are not unique because of the linear dependence of both friction force generalized directions in the wheel axis direction. If the actuated mechanical system is considered then one observes that the system is fully actuated when it moves in the two-DOF mode, in the other modes it is an underactuated system with less actuators than mechanical degrees of freedom. The transitions among all four operating modes are possible. The structure of the dynamics indicates that the accelerations $\ddot{\Psi}_{\mathrm{R}}$ and $\ddot{\Psi}_{\mathrm{L}}$ are decoupled from the accelerations of the chassis translational and angular accelerations. The structure of D_{s} clearly indicates that the underactuated chassis DOF x, y, ϕ are driven by the contact friction forces. The control torque is transferred, via set-valued coupling to the underactuated part of the dynamics.

Modes	${}_{\mathrm{K}}\boldsymbol{\gamma}_{Rx}$	${}_{\mathrm{K}}\boldsymbol{\gamma}_{Ry}$	${}_{\mathrm{K}}\boldsymbol{\gamma}_{Lx}$	${}_{\mathrm{K}}\boldsymbol{\gamma}_{Ly}$
5-DOF mode	$\neq 0$	$\neq 0$	$\neq 0$	$\neq 0$
3R-DOF mode	$= 0$	$\neq 0$	$= 0$	$= 0$
3L-DOF mode	$= 0$	$= 0$	$= 0$	$\neq 0$
2-DOF mode	$= 0$	$= 0$	$= 0$	$= 0$

Table 1. Relation of different modes to the contact state and relative contact velocities.

4 Numerical Results

In this section four maneuvers are presented where the robotic system undergoes explicit-phase transitions. In the first Maneuver B the system is expected to go energy-optimally from one point to another. In Maneuver A a time-optimally parking maneuver with a high dynamical action in the orientational DOF ϕ of the robot is required. In all maneuvers the robot is expected to start from standstill at the origin. The control moments of both wheels are limited to $\|M_{\mathrm{L}}\| = 1\,Nm$ and $\|M_{\mathrm{R}}\| = 1\,Nm$, respectively. A number of 300 discretization points are used and the controls are discretized with 60 points each.

4.1 Maneuver A

The desired end state to be reached time-optimally is given by:

$$\left(x_{\mathrm{f}},\, y_{\mathrm{f}},\, \phi_{\mathrm{f}},\, \psi_{\mathrm{Lf}},\, \psi_{\mathrm{Rf}}\right) = \left(1,\, 5,\, -\tfrac{\pi}{2},\, free,\, free\right).$$

Maneuver A is characterized by a high dynamical activity in the orientation of the chassis. The robot accomplishes this task in 4.03 seconds and the squared sum of the control effort is $1.8630\,N^2\,m^2 s$. In order to orient itself to $\phi = -\frac{\pi}{2}$ time-optimally in the final part of the maneuver the system performs a swing in maneuver during which it is in a five-DOF mode. At the beginning the system rushes onto trajectory in the vicinity $x = 1$ and swings counterclockwise out in order to have enough angular displacement to perform the swinging in the clockwise direction as can be seen in fig. (4).

4.2 Maneuver B

In Maneuver B the task is to reach the following endpoint control-effort optimally. The sum of squares of the actuating torques is being minimised. The desired end state to be reached is

$$\left(x_{\mathrm{f}},\, y_{\mathrm{f}},\, \phi_{\mathrm{f}},\, \psi_{\mathrm{Lf}},\, \psi_{\mathrm{Rf}}\right) = \left(1,\, 5,\, -\tfrac{\pi}{2},\, free,\, free\right).$$

The robot accomplishes this task in 4.05 seconds. As can be seen in figure (5) the CM of the robot traces a relatively straight line until the final reorientation maneuver during which dissipates kinetic energy during sliding as seen in fig. (5). As a consequence the mechanical system moves more in the non-dissipative two-DOF mode. In comparison to the control-effort Maneuver B, in maneuver A the robot moves more in the dissipative mode as seen in figures (8) and (9). The evolution of the center of mass trajectories in the x-y plane for maneuvers A and B can be seen in figures (10) and (11), respectively. The evolution of endtime t_{f} over the successive minimization of the augmented Lagrangian in both cases are depicted in figures (6) and (7), respectively.

4.3 Maneuver C

In maneuver C the task is to reach the following endpoint control-effort optimally. The sum of squares of the actuating torques is being minimised. The desired end state to be reached is

$$\left(x_{\mathrm{f}},\, y_{\mathrm{f}},\, \phi_{\mathrm{f}},\, \psi_{\mathrm{Lf}},\, \psi_{\mathrm{Rf}}\right) = \left(0,\, 5,\, 0,\, free,\, free\right).$$

As can be seen in figure (12) the CM of the robot does not trace a straight line but traces a curvilinear trajectory. In the second part of the maneuver, the robot moves more in the dissipative five-DOF mode and spends less effort to track the line connecting the initial and final points. The devation from the straight-line arises from the asymmetric loading condition of the robot, leading to unequal left and right wheel normal forces at standstill.

4.4 Maneuver D

In maneuver D the task is to reach the following endpoint control-effort optimally. The sum of squares of the actuating torques is being minimised. The desired end state to be reached is

$$\left(x_{\mathrm{f}},\, y_{\mathrm{f}},\, \phi_{\mathrm{f}},\, \psi_{\mathrm{Lf}},\, \psi_{\mathrm{Rf}}\right) = \left(0,\, 5,\, 0,\, free,\, free\right).$$

As can be seen in figure (13) the CM of the robot does race a straight line and the dissipative modes are avoided. As a consequence the mechanical system moves more in the nondissipative two-DOF mode and spends effort to track the line connecting the initial and final points.

5 Discussion and Conclusion

A numerical method is presented for the determination of optimal trajectories for switching Lagrangian systems. The Measure-Differential Inclusion (MDI) approach enables to consider simpler transition conditions by passing from the representation from acceleration level to velocity level so that the contact index sets are changed. The event-driven nature of the optimization problem is circumvented, by considering each discretization time point as a possible transition time where the system changes from one $x \in \mathcal{I}_M$ to any

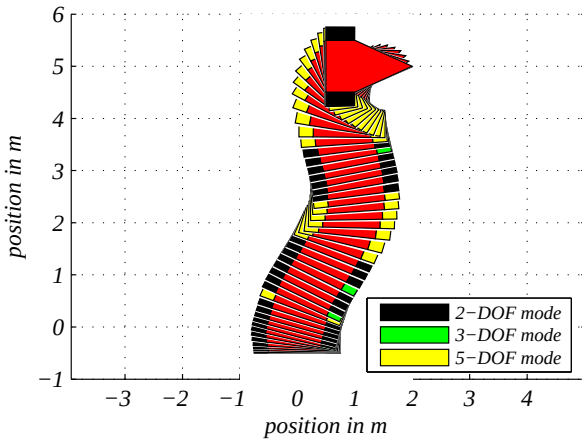

Figure 4. Maneuver A: Number of DOF during the maneuver.

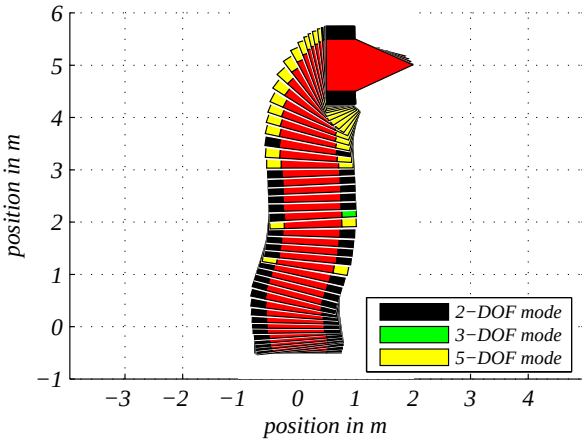

Figure 5. Maneuver B: Number of DOF during the maneuver.

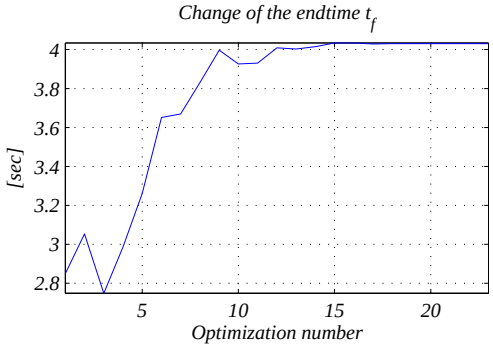

Figure 6. Maneuver A: The endtime t_f during successive minimizations.

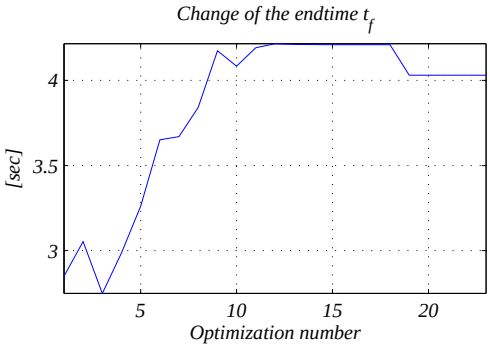

Figure 7. Maneuver B: The endtime t_f during successive minimizations.

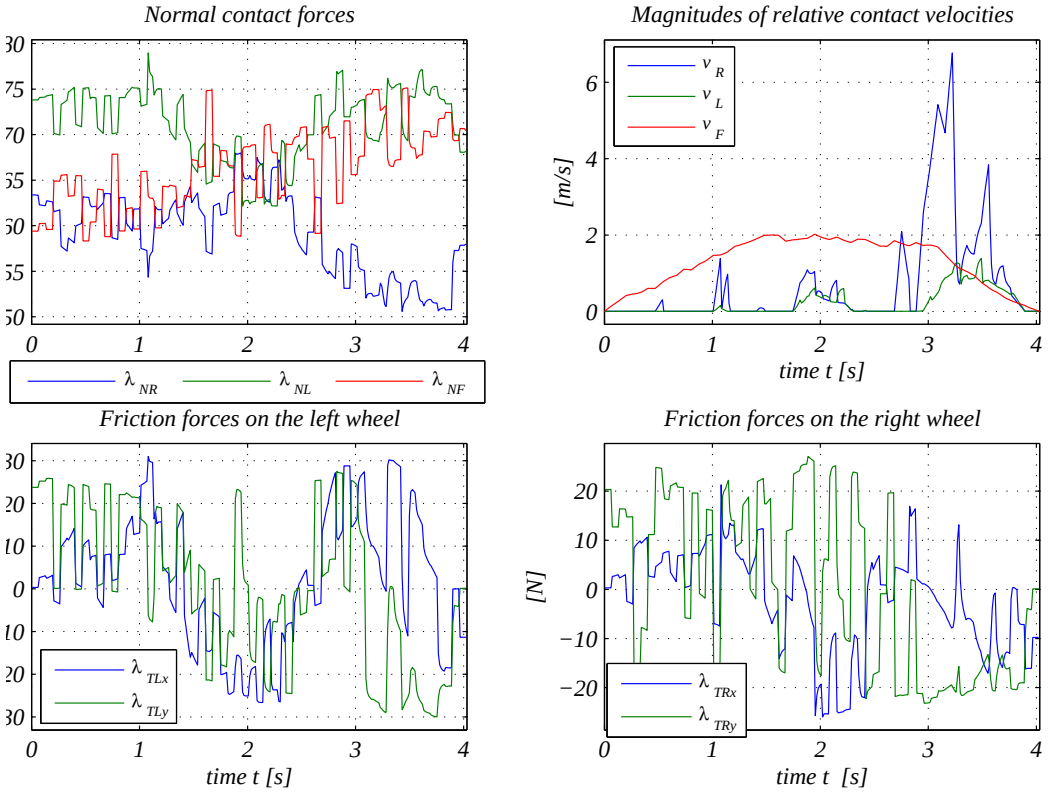

Figure 8. Maneuver A: Contact forces and contact relative velocities.

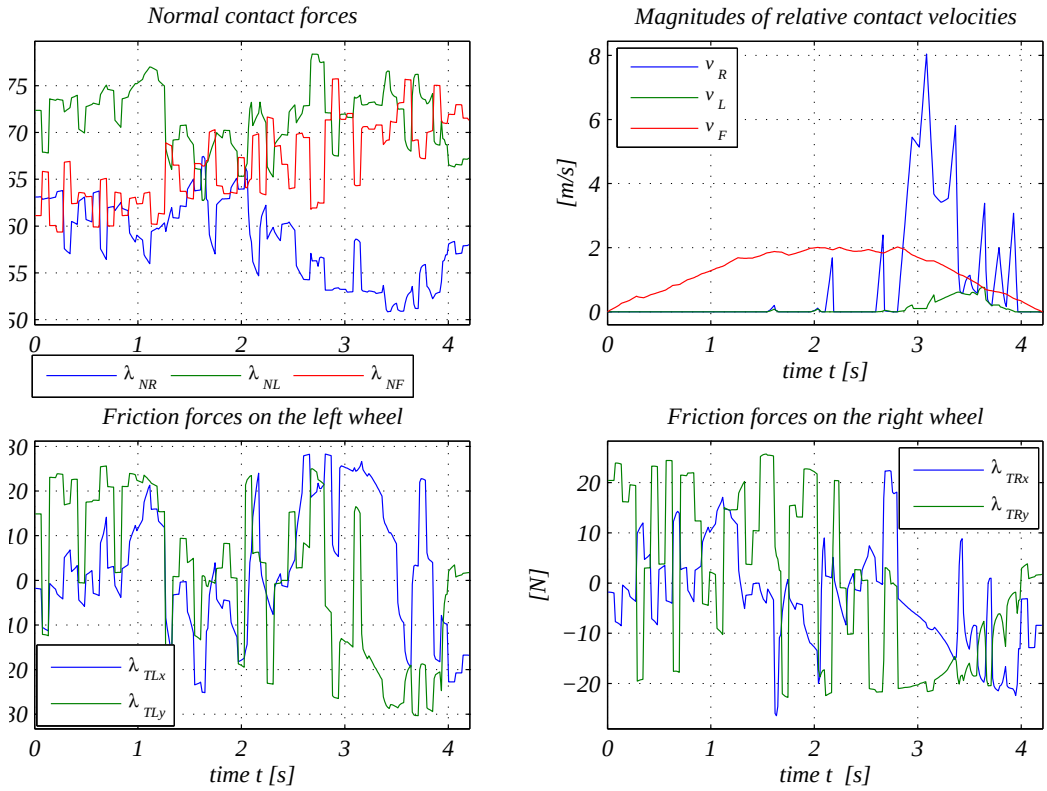

Figure 9. Maneuver B: Contact forces and contact relative velocities.

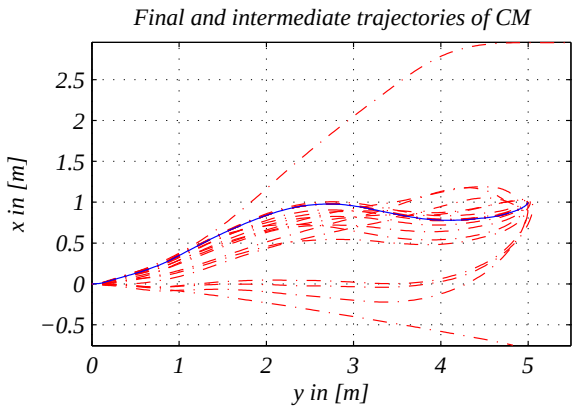

Figure 10. Maneuver A: The evolution of the trajectory of the CM.

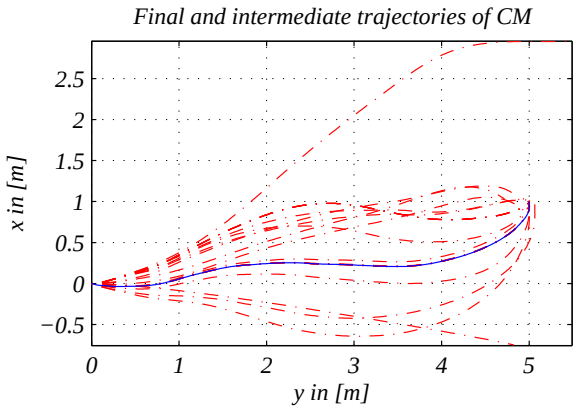

Figure 11. Maneuver B: The evolution of the trajectory of the CM.

another $y \in \mathcal{I}_M$. The resulting novel feature is that contrary to other shooting schemes for optimization problems with different phases, characterized by different system dynamics, multiple shooting is not necessary and the parameters of event or phase transitions need not to be optimized separately in the optimization. The proposed optimization scheme determines overall possible hybrid executions that lead to the final destination of switching Lagrangian system an at least locally-optimal solution. As a consequence, the location and time of phase transitions where the system changes DOF is not pre-specified but is determined as an outcome of the optimization. Following features of the MDI approach are important:

a The index sets that are used to take account of the behaviour of contacts on different levels such as position, velocity and acceleration for stick-slip transitions etc. is not managable for large systems with many contacts.

b The impacts, that may occur with or without collisions e.g. Painleve Paradox, velocity jumps due to C^0 constraints are a strong incentive to describe the mechanical systems as MDI, where the need is removed to consider transitions on acceleration level.

c As a novel property, the location and time of phase transitions where the system changes DOF is not prespecified but is determined as an outcome of the

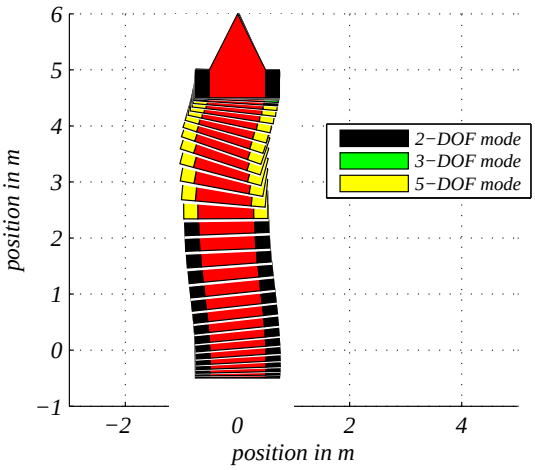

Figure 12. Maneuver C: Number of DOF during the maneuver.

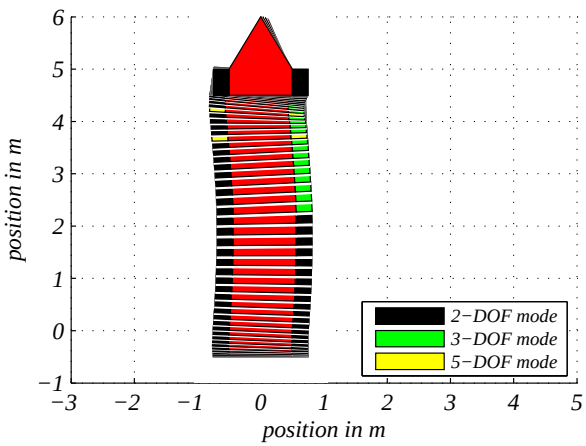

Figure 13. Maneuver D: Number of DOF during the maneuver.

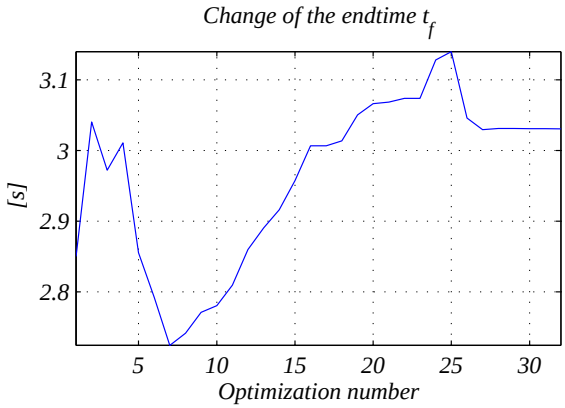

Figure 14. Maneuver C: The endtime t_f during successive minimizations.

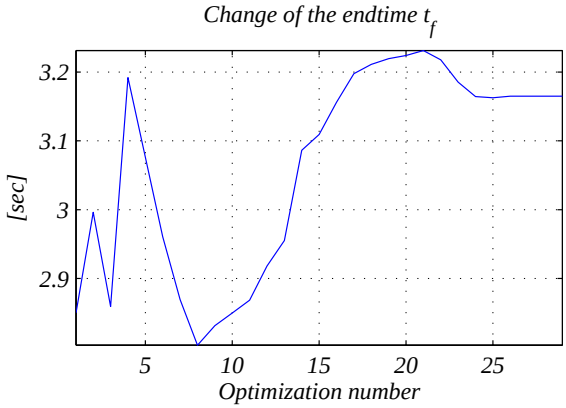

Figure 15. Maneuver D: The endtime t_f during successive minimizations.

optimisation. Though the underlying system might undergo structure-variant phase changes such as impactive phase transitions a mixed integer approach is not necessary. This is due to the fact that in this modeling framework every instant is equipped with the means to become a transition instant.

A Appendix

${}_\mathrm{K}\mathbf{r}_\mathrm{OA}$	vector pointing from O to A in system K
S_K	The center of mass the Chassis
S_L	The center of mass left wheel
S_R	The center of mass right wheel

Table 2. Notation

The inertia operators of each rigid-body is given as follows:

$$ {}_\mathrm{R}\Theta^{\mathbb{R}}_{S_\mathrm{R}} = {}_\mathrm{L}\Theta^{\mathrm{L}}_{S_\mathrm{L}} = \begin{bmatrix} a & 0 & 0 \\ 0 & b & 0 \\ 0 & 0 & b \end{bmatrix}, \tag{38} $$

$$ {}_\mathrm{K}\Theta^{\mathrm{K}}_{S_\mathrm{K}} = \begin{bmatrix} k_{11} & k_{12} & k_{13} \\ k_{21} & k_{22} & k_{23} \\ k_{31} & k_{32} & k_{33} \end{bmatrix}. \tag{39} $$

References

Alart, P. and Curnier, A. (1991). A mixed formulation of frictional contact problems prone to newton-like solution methods. *Computer Methods in Applied Mechanics and Engineering*, **92**, 353–375.

Moreau, J. J. (1999). Numerical Aspects of the Sweeping Process. *Computer Methods in Applied Mechanics and Engineering*, **177**, pp. 329–349.

Moreau, J. J. (1988). Unilateral Contact and Dry Friction in Finite Freedom Dynamics. In *Non-smooth Mechanics and Applications*, CISM Courses and Lectures. textbf302 Springer Verlag Wien.

m_{R}	mass of right wheel $[kg]$	0.287
μ	friction coeff. at wheels	0.4
m_{L}	mass of left wheel $[kg]$	0.287
μ_{f}	friction coeff. at stick	0.01
m_{K}	mass of chassis $[kg]$	19.466
r	wheel radius $[m]$	0.0385
f_{x}	x-comp. of ${}_{\mathrm{K}}\mathbf{r}_{S_{\mathrm{K}}S_{\mathrm{F}}}$ $[m]$	0.00876
f_{y}	y-comp. of ${}_{\mathrm{K}}\mathbf{r}_{S_{\mathrm{K}}S_{\mathrm{F}}}$ $[m]$	0.1794
f_{z}	z-comp. of ${}_{\mathrm{K}}\mathbf{r}_{S_{\mathrm{K}}S_{\mathrm{F}}}$ $[m]$	-0.0473
$\mathbf{r}_{\mathrm{x}}$	x-comp. of ${}_{\mathrm{K}}\mathbf{r}_{S_{\mathrm{K}}S_{\mathrm{R}}}$ $[m]$	0.168
$\mathbf{r}_{\mathrm{y}}$	y-comp. of ${}_{\mathrm{K}}\mathbf{r}_{S_{\mathrm{K}}S_{\mathrm{R}}}$ $[m]$	-0.09
$\mathbf{r}_{\mathrm{z}}$	z-comp. of ${}_{\mathrm{K}}\mathbf{r}_{S_{\mathrm{K}}S_{\mathrm{R}}}$ $[m]$	-0.0088
l_{x}	x-comp. of ${}_{\mathrm{K}}\mathbf{r}_{S_{\mathrm{K}}S_{\mathrm{L}}}$ $[m]$	0.0906
l_{y}	y-comp. of ${}_{\mathrm{K}}\mathbf{r}_{S_{\mathrm{K}}S_{\mathrm{L}}}$ $[m]$	-0.15
l_{z}	z-comp. of ${}_{\mathrm{K}}\mathbf{r}_{S_{\mathrm{K}}S_{\mathrm{L}}}$ $[m]$	-0.0088
a	wheel inertia $[kg\,m^2]$	1.6778×10^{-4}
b	wheel inertia $[kg\,m^2]$	1.5604×10^{-4}
k_{11}	chassis inertia $[kg\,m^2]$	0.3646
k_{12}	chassis inertia $[kg\,m^2]$	0.0372
k_{13}	chassis inertia $[kg\,m^2]$	0.026
k_{21}	chassis inertia $[kg\,m^2]$	0.0372
k_{22}	chassis inertia $[kg\,m^2]$	0.2505
k_{23}	chassis inertia $[kg\,m^2]$	1.46×10^{-4}
k_{31}	chassis inertia $[kg\,m^2]$	0.026
k_{32}	chassis inertia $[kg\,m^2]$	1.46×10^{-4}
k_{33}	chassis inertia $[kg\,m^2]$	0.4306

Table 3. Numerical values of physical parameters of the robot.

Glocker, Ch. (2001). *Set-Valued Force Laws- Dynamics of Non-Smooth Systems*. Volume 1 of Lecture Notes in Applied Mechanics. Springer Verlag.

Rockafellar, R. T. (1974). Augmented Lagrange Multiplier Functions and Duality in Nonconvex Programming. *SIAM J. Control*, **12**(2), pp. 268–285.

Rockafellar, R. T. (1976). Augmented Lagrangians and Applications of the Proximal Point Algorithm in Convex Programming. *Mathematics of Operations Research*, **1**(2), pp. 97–116.

Rockafellar, R. T. (1981). Proximal Subgradients, Marginal Values and Augmented Lagrangians in Nonconvex Optimization. *Mathematics of Operations Research*, **6**(3), pp. 424–436.

Yunt, K. and Glocker, Ch. (2005). Time-Optimal Trajectories of a Differential-Drive Robot. In *Proc. of the fifth EUROMECH Nonlinear Dynamics Conference*, ENOC 2005 Eindhoven, Netherlands, pp. 1589–1596.

Yunt, K. (2006). Trajectory Optimisation of Structure-Variant Mechanical Systems. In *IEEE Proc. of 9th Int. Workshop on Variable Structure Systems*, VSS 2006 Alghero, Italy, pp. 298–303.

Yunt, K. and Glocker, Ch. (2007). Modeling and Optimal Control of Hybrid Rigidbody Mechanical Systems. In *Hybrid Systems Computation and Control Lecture Notes in Computer Science 4416*, HSCC 2007, Springer, pp. 614–627.

Xu, X. and Antsaklis, P.J. (2002). Optimal Control of switched systems via non-linear optimisation based on direct differentiations of value functions. *Int. J. Control*, **75**(16/17), pp. 1406–1426.

Xu, X. and Antsaklis, P. J. (2002). Optimal Control of Switched Autonomous Systems. In *IEEE Proc. of the 41st IEEE Conference on Decision and Control*, pp. 4401–4406.

Murphey, T. (2002). Control of Multiple Model Systems. PhD Thesis, California Institute of Technology.

Anitescu, M. and Florian, A. P. (2001). A time-stepping method for stiff multibody dynamics with contact and friction. *Int. Journal for Num. Meth. in Engr.*, **55**, pp. 753–784.

Studer, C. and Glocker, Ch. (2006). Representation of normal cone inclusion problems in dynamics via non-linear equations. *Archive of Applied Mechanics*, **76** (5-6), pp. 327–348.

Studer, C. and Glocker, Ch. (2006). Solving normal cone inclusion problems in contact mechanics by iterative methods. *Journal of System Design and Dynamics*, **1** (3, Special Issue on the Third Asian Conference on Multibody Dynamics 2006), pp. 458–467.

Stewart, D. E. and Trinkle, J. C. (1996). An Implicit Time-Stepping Scheme for Rigid-Body Dynamics with Inelastic Collisions and Coulomb Friction. *Int. Journal for Num. Meth. in Engr.*,**39** , pp. 2673–2691.

Egerstedt, M., Wardi, Y. and Axelsson, H. (2006). Transition-time Optimisation for Switched-Mode Dynamical Systems. *IEEE Trans. in Automatic Control*, **51** (1) , pp. 110–115.

Egerstedt, M., Wardi, Y. and Delmotte, F. (2003). Optimal Control of Switching Times. In *IEEE Conference on Decision and Control*.